Colloquia: FATA 2019

US/TOF-PET endorectal probe compatible with MR, for diagnosis and staging of the prostate cancer

F. Garibaldi([1]), V. Bettinardi([2]), G. Brembilla([2]), A. Briganti([2]),
E. Cisbani([3]), N. Clinthorne([4]), F. De Cobelli([2]), C. de la Taille([5]),
M. Fournelle([6]), L. Gianolli([2]), S. Majewski([7]), F. Montorsi([2]),
J. Nuyts([8]), M. Picchio([2]) and K. Ziemons([9])

([1]) *Istituto Nazionale di Fisica Nucleare, Sezione di Roma - Roma, 00185 Italy*
([2]) *Università Vita e Salute S. Raffaele - Milano, 20132 Italy*
([3]) *Istituto Superiore di Sanità - Roma, 00161 Italy*
([4]) *Dept. Radiology, University of Michigan - Ann Arbor, MI 48109-5610, USA*
([5]) *Omega Lab, École Polytechnique, CNRS/IN2P3 - Saclay, France*
([6]) *Fraunhofer-Institute - Sulzbach, 66386 Germany*
([7]) *University of California - Davis, One Shields Avenue, CA 95616, USA*
([8]) *KU Leuven University - UZ Herestraat 49, 3000 Leuven, Belgium*
([9]) *FH Aachen - Heinrich-Mußmann-Strasse 1, Jülich, 52428 Germany*

Summary. — Prostate Cancer (PCa) is one of the most prevalent cancers worldwide. Early and accurate diagnosis of PCa is crucial for effective and successful treatment. Our project aims at developing a unique, highly performing flexible geometry multi-modality imaging system for diagnosis and staging of PCa. The imager will have the form of an endorectal probe combining high-resolution (0.1 mm) ultrasound (US) with a very high-resolution Positron Emission Tomography (PET) probe (1 mm spatial resolution) with exceptional Time-of-Flight (TOF) capability (100 ps FWHM targeted) compatible with Magnetic Resonance Imaging (MRI), in coincidence with a set of external PET panels. While standard multiparametric MRI (mpMR) has drawbacks, diagnosis will be improved significantly by the introduction of PSPMA-PET as well as the simultaneous PET/MR imaging. The system will be capable of morphological visualization instantly and continuously combined with biological and metabolic activity, offering crucial improvement with respect to standard systems (detection of ~ 2 mm lesions *vs.* ~ 6 mm lesions) in spatial resolution, efficiency, signal-to-noise ratio (SNR), scanning time and/or lowering injected dose.

1. – The present status of diagnosis of prostate cancer

Prostate Cancer (PCa) is one of the most prevalent cancers worldwide [1]; early and accurate diagnosis is crucial for successful treatment. The extent of PCa (prostate, extracapsular, seminal vesicles) as well as risk stratification as determined by histological differentiation (Gleason score) of PCa lesions significantly influence further treatment decisions. Globally, the majority of urology departments still utilize low-resolution US probes, in conjunction with PSA and Digital Rectal Examination (DRE), to help diagnosis and guide biopsy. However it is not very accurate.

Multi-parametrical MR (mpMRI) is increasingly exploited in the diagnosis of PCa and is becoming the imaging modality of choice for it [1-5]. mpMRI information can then be used for histological verification of suspicious lesions [4] by means of "fusion biopsy" (US+mpMRI) [6], recommended by leading urologic guidelines [1]. However mpMRI has severe drawbacks. The main source of error in MRI leading to false negatives are sparse and diffuse peripheral tumors [7-10]. Lesions can be overlooked [10]. Both low-grade and high-grade Gleason score lesions (small, even <1 cm, and large) have serious limitations in being detected by mpMRI [11, 12].

Satellite lesions and peripheral lesions as well as small cancer foci (<0.5 cm^3) can be missed [11, 13, 14]. Moreover large inter-reader variations are accounted for [15]. A study shows that US-mpMRI is not able to detect lesions <3 mm [13] that might be malignant. Positron Emission Tomography (PET) with specific tracers (PSMA) significantly improved diagnosis of PCa, showing a higher specificity and sensitivity for the detection of tumor lesions compared to CT, MRI [2, 7, 8, 16]. It showed superior performance also in the identification of metastatic lymph-nodes (LNs) [17] and in biopsy guidance [18, 19]. Moreover it is a powerful diagnostic tool especially if combined with mpMR [12]; since mpMR and PET are imaging modalities based on different physical and biological principles, additional complementary benefit is obtained when they are combined [2, 7, 8, 16, 20, 21].

PET and MR have to be simultaneous [22, 23]. The human prostate is flexible and can be deformed under external conditions, such as patient position or the insertion of the PET probe, so the localization of the targeted imaging region under the same circumstances requires using simultaneous MRI and PET. Incorporation of PET/mpMRI into the workup and monitoring of patients with low-risk prostate cancer can help in discriminating clinically significant disease from indolent ones [24]; however also this hybrid method is not perfect and fails to detect microscopic lesions mainly due to the limited spatial resolution of the standard PET or PET-MR systems ($\sim$3.5 mm FWHM): a very important requirement for a hybrid detector system for diagnosis and staging of PCa is the capability of detecting very small lesions ($\sim$2–3 mm), missed by standard scanners.

2. – US/TOF–PET/MR proposed system

We propose a unique, innovative, multimodality molecular imaging system that will merge anatomical and functional details for diagnosis and staging of PCa. The system integrates, for simultaneous US/TOF–PET/MRI, high-resolution (0.1 mm) ultrasound (US) and, benefitting from the magnification PET geometry, a very high-resolution/high-efficiency PET probe in coincidence with very high-resolution/high-efficiency external PET panels with unprecedented Time-of-Flight (TOF) capability, placed close to the body of the of the patient [25]. Our target spatial resolution for the system is $\sim$1 mm.
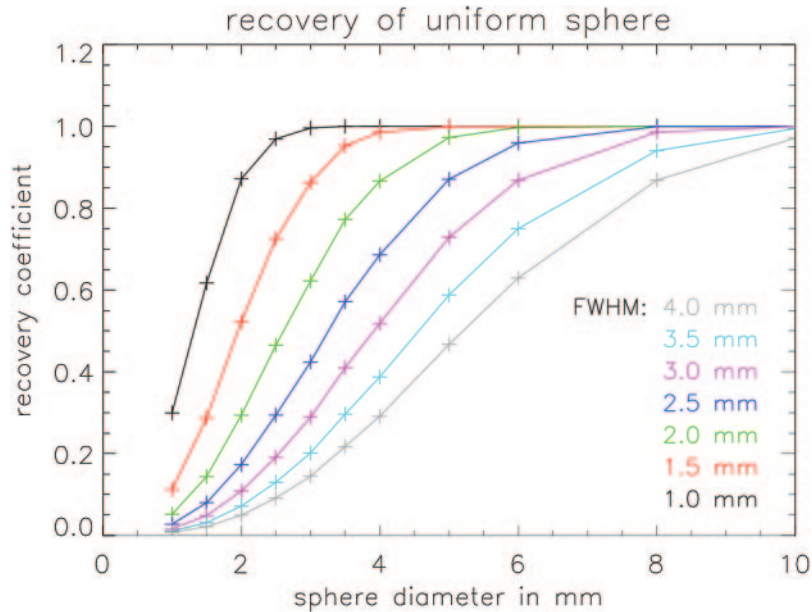
Fig. 1. – Evaluation of detection capability of small lesion as a function of lesion diameter and detector spatial resolution. The lesion is modeled by a sphere with uniform activity. The recovery coefficient (defined as the maximum value of the sphere in the reconstructed image, divided by the true value of the uniform sphere) is shown as a function of the sphere diameter for systems with different spatial resolution. For a 3 mm diameter sphere, the image contrast is increased with a factor of 5 when the system resolution is improved from 4 mm to 2 mm.

The detector system will exactly localize within the prostate even small PCa lesions missed with standard PET-MR scanners. It also offers the possibility of real-time diagnosis of suspicious tracer accumulations within the prostate by directly guiding targeted biopsies [18]. Adding high-resolution TOF-PET imaging to endoscopy is a real revolution of wide reach, important especially in the case of high background [26]. The system will be much cheaper and crucially more performant than the whole-body standard PET/MRI; it will be designed to operate, potentially, inside practically any MRI scanner with high potential for wide utilization.

Figure 1 shows the recovery coefficient (the ratio of the apparent tracer uptake in the image to the true tracer uptake) for spheres with different diameter (that mimic different lesions), as a function of the system resolution. This illustrates the importance of the system resolution for the detection and correct diagnosis of small lesions. Our proposed detector system ($\sim$1 mm resolution) will enable accurate imaging of spheres as small as 2 mm, whereas with current state of the art PET scanners (3.5 mm resolution), such spheres will appear as a small fluctuation in the background (fig. 1).

As seen previously it is highly desirable [27] to detect lesions as small as 2 mm not within reach of the best standard detectors. Better PET performances are needed: spatial and TOF resolution, efficiency, all of them impacting the Signal-to-Noise Ratio (SNR) strongly related to the lesion detectability. In this respect, fig. 2 illustrates the impact of resolution improvements on the amount of information that the PET system acquires about the difference between a small hot lesion and a larger but far less hot region.
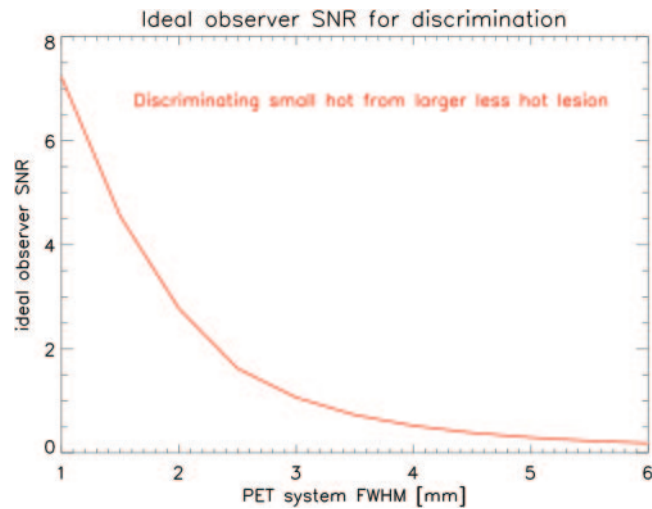
Fig. 2. – An ideal observer study was done to quantify the amount of information for discriminating two lesions, provided by PET projections with a particular spatial resolution. Lesion 1 had a 2 mm diameter and tissue-to-background ratio of 5, lesion 2 had a 3.5 mm diameter and a tissue-to-background ratio of 1.75. The information was quantified as the SNR of the ideal observer. It is observed that improving the system resolution from 4 mm to 2 mm leads to a 5.3 fold SNR improvement. Discrimination of such lesions is expected to be clinically relevant for prostate imaging with PSMA-PET.

As is shown in the figure, the SNR of the ideal observer increases with a factor of more than 5 for the discrimination between a lesion with a tissue-to-background value of 5 (which would be considered very suspicious in PSMA imaging) and a larger lesion with tissue-to-background ratio of 1.75 (which could be normal or benign uptake).

2˙1. *The endorectal probe*. – The probe and a schematic layout of the system are shown in fig. 3. The detector system will allow the simultaneous acquisition of PET/MRI images. We will use LYSO or LSO doped with calcium as scintillator material for the PET
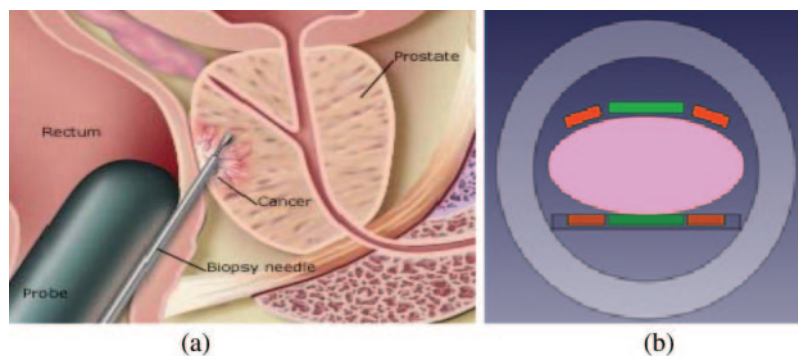
Fig. 3. – (a) Relevant anatomic details. (b) The layout of the PET probe used with dedicated PET external panels. The PET system uses coincidences between the internal detector (probe) and the external panels as well as coincidences between the panels [28].
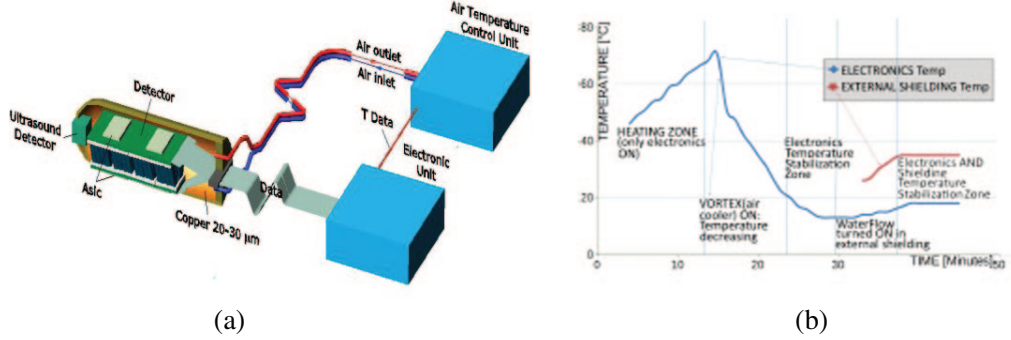
Fig. 4. – (a) The layout of the endorectal probe. (b) Stabilization of the internal and external probe temperatures.

detectors. The dimension of the pixelated scintillator is $\sim 25 \times 50 \times 13\,\mathrm{mm}^3$. The scintillator pixels ($1 \times 1\,\mathrm{mm}^2$) will be coupled one to one double side to the SiPM pixels in order to optimize light collection for spatial and timing resolution and Depth of Interaction (DOI) [29, 30]. Silicon PhotoMultipliers (SiPM) will be used as photodetectors (Hamamatsu SiPM S13615-1050N-08, or better ones if they appear on the market). They are compact, insensitive to magnetic fields and have very good timing properties [31].

The layout of the detection probe is shown in fig. 4(a) [25]. The probe cage is a cylinder with external diameter of 35 mm. Cool air will be used for the electronics; water flow in the interstices of the container will allow stabilizing the external temperature of the probe (fig. 4(b)); we will consider other options like warm air cooling and very effective insulators [32]. We will choose the most effective and the safest one.

All selected materials will be biocompatible with the human body [33] according to current regulations and non-magnetic to be compatible with MRI scanners. Shielding of the RF field to the PET electronics is needed to minimize the effect of eddy currents. A Korean group did a detailed study of thickness, area and open area of a copper mesh, as a function of the relative position of PET detector and RF coil on MRI [34]. Cherry's group found that carbon fiber composite material was a good RF shield at the Larmor frequency while introducing negligible gradient Eddy currents [35]. Moreover Ziemons and collaborators proposed the separation into two areas but linked via high-value capacitors [36].

A high-resolution US sensor will be installed in front of the PET probe for position tracking, to assure high-resolution imaging and accurate guiding [37-39] of biopsy. Optical and MR tracking systems will be considered in order to know the exact position and direction of the probe with respect to the PET panels and the prostate [40-43]. We will choose the best for accuracy and practical reasons.

2$^{\cdot}$**2.** *External TOF-PET panels.* – Angular coverage sufficient to get artefact free images will be needed for a given TOF resolution; the better the TOF resolution, the smaller the coverage necessary [44]. We will use $(4 + 4)$ external PET panels on the opposite sides of the pelvic region of the patient (each panel has an area of $\sim 100 \times 250 \times 20\,\mathrm{mm}^3$) with scintillator pixels of $2 \times 2\,\mathrm{mm}^2$ coupled one to one (double sides to optimize DOI) to SiPM of the same pitch.

The layout and the pixel size are chosen as the best compromise to obtain excellent spatial resolution, efficiency and TOF resolution (because of their small capacitance). The analysis of data from phantom and clinical trial will be analyzed with single- and

double-side coupling of scintillators with SIPM in order to evaluate the DOI and its impact on the image quality. The analysis will be performed at full and reduced angular coverage, *e.g.*, 4 + 4 and less PET panel configuration to know the optimal solution performance/complexity/cost.

2˙3. *Time of Flight (TOF)*. – The time-of-flight information (*i.e.*, arrival time difference of the detected photons) allows reducing the uncertainty in the localization of the annihilation place along the line connecting the pixels/crystals fired in coincidence. Time resolution of the best scanner is <250 ps (FWHM) range, translating into ∼3.75 cm (FWHM) positional uncertainty. With 100 ps the positional uncertainly would be ∼1.5 cm [26, 45].

Timing resolution depends on several parameters like scintillator properties (light output, timing), path length spread (light collection), transit time in the photodetector, TDC time spread, discriminator time spread, system noise contributions (power supply, clocks, cables). All of these contributing factors will be optimized: one-on-one coupling of scintillator pixels with SiPMs, using SiPMs with low capacitance, and a new ASIC. So a timing resolution of 100 ps will be possible.

For the center of a uniform object which is large compared to the TOF uncertainty, improving the TOF resolution by a particular factor results in a decrease of noise variance in the reconstructed image by the same factor. As a result, the SNR increases by the square root of that factor.

Table I shows the improvement of SNR as a function of the timing resolution. The excellent TOF resolution will allow us to have PET images almost free from artefact despite incomplete angular coverage [44] and will facilitate attenuation correction [46]. Preliminary results from our team show that a detector with very good planar and DOI (<1 mm) resolutions and with good TOF resolution can be realized [25, 29, 30].

2˙4. *The new ASIC and electronics to improve TOF resolution*. – The proposed system requires very compact electronics and a dedicated multi-channel ASIC for fast timing. SiPM detectors benefit from a large deposited charge and a very short current pulse (<100 ps) but suffer from large sensor capacitance. To cover large areas with excellent timing resolution it is therefore necessary to match sensor size and readout electronics.

The preamplifier need to be optimized in order to obtain the largest bandwidth while taking into account the connection to the sensor. This will require minimizing the stray inductance and will be achieved by using a flip chip technique. The chip will comprise 64 channels of innovative preamplifier and high-speed discriminator, coupled to low-power

TABLE I. – *Improvement of SNR and NEC as a function of the timing resolution.*

Time resolution (ns)	Δx (cm)	TOF noise var gain	TOF SNR gain
0.1	1.5	26.7	5.2
0.3	4.5	8.9	3.0
0.6	9.0	4.4	2.1
1.2	18.0	2.2	1.5
2.7	40.0	1.0	1.0

time-to-digital converters; digital processing will allow output the data at high Gb/s speed.

The new ASIC design will strongly benefit from the experience gained by the group in developing challenging ASIC for particle physics. Specifically it is proposed to adapt the preamplifier to SiPM signals exploiting the RF architecture used in PETIROC [47] and adapt the advanced ALTIROC [48,49] design to the TOF-PET readout. The former chip, targeted to TOF application, reads 32 SiPM channels with 1 GHz bandwidth that feature an 18 ps RMS jitter with 4 photoelectron threshold. Internal ADCs and TDCs provide digitized charge and time information for channels above threshold. The power dissipation of 200 mW and TFBGA 12×12 mm package allow mounting it very close to the sensors [50]. The latter ALTIROC new-generation 130 nm CMOS chip relies on advanced high-speed ASIC for 10 ps timing on large areas of LGAD diodes.

$2\dot{}5$. *The high-resolution compact US device*. – US imaging systems for TRUS work in the 5–10 MHz with resolutions of several hundred μm. There is a trade-off between resolution and penetration depth in ultrasound, since acoustic damping is strongly frequency-dependent. MicroUS (μUS) has been lately made available. Lower penetration depths are required in prostate imaging compared to other organs so higher frequencies providing better resolution can be used. We will achieve further and significant progress with μUS devices by introducing high-pitched ultrasound arrays pushing the resolution limit towards 100 μm. Such arrays will be integrated within very small volumes using extremely small interconnects to external imaging instrumentation, allowing us to integrate it in the PET probe. The μUS devices will be optimized to allow penetration through the full depth of the prostate with the best possible spatial resolution, providing, potentially, also additional diagnostic information. Shear wave elastography which gives access to the tissue stiffness that has been demonstrated to be an indicator for tissue malignancy [37-39] will be supported.

$2\dot{}6$. *PET/MRI compatibility*. – It has been shown that both modalities preserve their functionality, even when operated isochronously [51]. The average MR image SNR showed small degradations when the PET insert was put in the magnet [52]. We performed measurements with our prototype of the prostate probe in a 4.7 T scanner [25]. Test results showed that overall the PET device does not cause a significant loss of the MR signal to noise and therefore would not prevent the simultaneous use of both the MRI coil and the PET device within a clinical scanner [25].

$2\dot{}7$. *Endorectal MR coil*. – MR imaging with endorectal coil (ERC) in local staging of prostate cancer is debated extensively in the literature [50]. It is undisputed that SNR and spatial resolution are significantly better by the use of an ERC imaging technology than a standard pelvic phase array coil [53]. Moreover, a number of studies have demonstrated improvements in the detection quality and localization accuracy using the endorectal type of coils relative to other methods [53-55].

Despite the clear advantages of using hybrid MR-PET systems, there are technical challenges to be taken into account. For example the efficiency of the RF coil could be affected from the needed shielding of the PET probe; some effect could be induced on the MR image. However it has been shown by Choi and Ziemons that with a careful choice of the coil both the MR and PET images are excellent [36]. Based on this result, we will exploit this knowledge to design and build an ERC detector system as indicated in [36].

2˙8. *Reconstruction software*. – Development of dedicated high-resolution PET image reconstruction software for accurate and precise images of the prostate is a challenging objective that will require novel TOF reconstruction algorithms for the proposed PET detection system (flexible geometry with limited angular coverage). This software will use the available probe position information, provided by the passive tracking arm, to calibrate the particular PET system geometry that changes with the changing position of the endorectal probe. It will include correction for photon attenuation and Compton scatter [40, 41] either based on the MR-based attenuation map (MRAC) or, if the PET system is operated outside the MR, using attenuation estimates obtained from the TOF-PET data themselves [56, 57]. In addition, based on the geometry, and, if necessary, on joint estimation techniques applied to the TOF-PET data, it will estimate the detector-pair sensitivities [46, 58-61]. Due to these corrections, images of good visual and quantitative quality will be obtained.

3. – Preclinical tests and plot clinical trials

Once all the above components have been integrated into a demonstrator system, it will undergo extensive preclinical tests before final clinical trials.

In the first step we will use solid positron emitting point sources placed within a gel matrix and the detection capability of these sources by the PET component of the developed prototype will be evaluated. For phantom evaluation a multi-modality prostate training phantom will be prepared to contain inserts of ^{68}Ga or ^{18}F or other positron emitters. After imaging using a standard PET/MR scanner the phantom will be imaged by the developed system with position tracking to generate a 3D-image volume.

The validity of the new system data will be evaluated by a comparison with PET/MR images. In the third step the biopsy guidance fixture will be attached to the developed endorectal probe system and bioptic puncture of the radioactive lesions will be performed. Image reconstruction and fusion as well as needle tracking will be fully operational during these tests.

The accuracy of the novel system will be then assessed in a pilot clinical trial. A total of 50 patients with clinically localized prostate cancer undergoing radical prostatectomy will be identified. All patients will subsequently undergo a study with the Signa PET/MR scanner with phase array coil. All patients will be preoperatively evaluated using the novel system with endorectal and phase array coils at least 6 weeks after prostate biopsy. Fusion biopsy will be performed adding the PET probe images to the mpMRI ones. Then all patients will be treated with a robot-assisted radical prostatectomy with or without lymph-node dissection according to disease characteristics. All resected specimens will be analyzed by expert high-volume uro-pathologists.

The primary endpoint will be represented by the detection of clinically significant prostate cancer, defined as the presence of lesions with Gleason score $\geq 3 + 4$ at final pathology. Secondary endpoints will be the detection of extracapsular extension and/or seminal vesicle invasion. The performance characteristics of the novel imaging method for the detection of clinically significant prostate cancer and for local staging will be assessed and compared with mpMRI and PET/mpMRI. The pathologic report will represent the gold standard.

The performance of the novel imaging system will be assessed for different outcomes in the overall population and after stratifying patients according to preoperative PSA values and Gleason score. The receiver operating characteristics area under the curve method will estimate the predictive accuracy of these methods.

4. – Conclusions and outlook

Our ambitious project main goal is the development of the high-resolution dedicated prostatic US/TOF-PET system, compatible with MRI, in order to improve:

- Lesion detectability through better signal-to-noise ratio (obtained also by dramatic suppression of partial volume effects) in detecting and discriminating small lesions with much higher spatial resolution PET system.

- Angular coverage needed to obtain (almost) artifact-free PET images and high sensitivity, and in consequence short scanning time, and/or low dose.

- Accuracy by which the attenuation correction can be estimated from TOF-PET data.

Such a complex system needs the careful evaluation of different configurations for optimization of performances, complexity, cost, within acceptable clinical requirements. The final demonstrator prototype will be used for preclinical tests to evaluate and validate its performance on phantoms, and then in clinical trials.

REFERENCES

[1] MOTTET NICOLAS *et al.*, *Eur. Urol.*, **71** (2017) 618.
[2] YILMAZ B. *et al.*, *The Prostate*, **79** (2019) 1007.
[3] TORRE L. A. *et al.*, *CA Canc. J. Clin.*, **65** (2015) 87.
[4] AHMED H. U. *et al.*, *Lancet*, **389** (2017) 815.
[5] MARGOLIS D. J. A. *et al.*, *BioMed. Res. Int.*, **2014** (2014) 684127.
[6] VALERIO M *et al.*, *Eur. Urol.*, **68** (2015) 8.
[7] PERERA M. *et al.*, *Eur. Urol.*, **70** (2016) 926.
[8] ABD ALKHALIK BASHA MOHAMMAD *et al.*, *Abdom. Radiol.*, **44** (2019) 2545.
[9] DIANAT S. S. *et al.*, *Urol. Oncol.*, **32** (2014) e1.
[10] TANEJA S. *et al.*, *Am. J. Roentgenol.*, **210** (2018) 1338.
[11] LE J. D. *et al.*, *Eur. Urol.*, **67** (2015) 569.
[12] RAHBAR K. *et al.*, *J. Nucl. Med.*, **57** (2016) 563.
[13] RASTINEHAD A. R. *et al.*, *J. Urol.*, **185** (2011) 815.
[14] SCHOUTEN M. G. *et al.*, *Eur. Urol.*, **71** (2017) 896.
[15] SONN G. A., *Eur. Urol. Focus*, **5** (2019) 592.
[16] HICKS R. M. *et al.*, *Radiology*, **289** (2018) 730.
[17] JILG C. A. *et al.*, *Theranostics*, **7** (2017) 1770.
[18] MAURER T. *et al.*, *Nat. Rev. Urol.*, **13** (2016) 226.
[19] EIBER M. *et al.*, *Eur. Urol.*, **70** (2016) 829.
[20] WESTENFELDER K. M. *et al.*, *Clin. Genitourinary Canc.*, **16** (2018) 245.
[21] MOTTAGHY F. M. *et al.*, *Eur. J. Nucl. Med. Mol. Imaging*, **43** (2016) 1397.
[22] BAILEY D. L. *et al.*, *Mol. Imaging Biol.*, **20** (2018) 4Y20.
[23] HERZOG HANS Z., *Med. Phys.*, **22** (2012) 281.
[24] DIANAT S. S. *et al.*, *Urol. Oncol.: Sem. Orig. Inv.*, **32** (2014) 39.
[25] GARIBALDI F. *et al.*, *Eur. Phys. J. Plus*, **132** (2017) 396.
[26] MOSES W. W., *Nucl. Instrum. Methods A*, **580** (2007) 919.
[27] TAN NELLY *et al.*, *Am. J. Roentgenol.*, **205** (2015) W87.
[28] VON EYBEN F. E. *et al.*, *Eur. Urol. Focus.*, **4** (2016) 686.
[29] COSENTINO L. *et al.*, *Rev. Sci. Instrum.*, **83** (2012) 114301.
[30] COSENTINO L. *et al.*, *Rev. Sci. Instrum.*, **83** (2012) 84302.
[31] RENKER D., *Nucl. Instrum. Methods A*, **567** (2006) 48.

[32] `https://m.indiamart.com/proddetail/super-multilayer-insulation-pads-90884121`
    `33.html`.

[33] Gagan Kaur *et al.*, *RSC Adv.*, **5** (2015) 37553 and `https://www.quadrantplastics.`
    `com/eu-en/industries/medical-life-science.html`.

[34] Kang Jihoon *et al.*, *2009 IEEE Nuclear Science Symposium Conference Record M13-261*
    (IEEE) 2009, `https://doi.org/10.1109/NSSMIC.2009.5401902`.

[35] Peng Bo J. *et al.*, *J. Magn. Reson.*, **239** (2014) 50.

[36] Choi C.-H. *et al.*, *Design, evaluation and comparison of RF surface coils for hybrid MR-
    PET imaging of the prostate*, to be published in *Phys. Med. Biol.*

[37] Rohrbach D. *et al.*, *Ultrasound Med. Biol.*, **44** (2018) 1341.

[38] Pavlovich C. *et al.*, *Urol. Oncol.*, **32** (2014) 34.e27.

[39] Wei C. *et al.*, *J. Urol.*, **200** (2018) 549.

[40] Maier-Hein L. *et al.*, *Proc. SPIE*, **6918** (2008) 1605.

[41] Elfring Robert *et al.*, *Comput. Aided Surg.*, **15** (2010) 1.

[42] Eschelbach Martin *et al.*, *Proc. Intl. Soc. Mag. Reson. Med.*, **25** (2017) 1304.

[43] Godenschweger F. *et al.*, *Phys. Med. Biol.*, **61** (2016) R32.

[44] Surti S. *et al.*, *Phys. Med. Biol.*, **53** (2008) 2911.

[45] Lecoq P., these Proceedings.

[46] Defrise M. *et al.*, *Phys. Med. Biol.*, **57** (2012) 885.

[47] Monzo J. M. *et al.*, *J. Instrum.*, **12** (2017) C02059.

[48] De La Taille C. *et al.*, PoS TWEPP-17 (2018) 006 AIDA-2020-CONF-2018-005 and
    CERN-LHCC-2018-023; LHCC-P-012.

[49] Omega-Centre de Microelectronic-Product Specs Web Site, `https://portail.poly`
    `technique.edu/omega/en/products/products-presentation`.

[50] Dickinson L. *et al.*, *J. Magn. Reson. Imaging*, **36** (2013) 48.

[51] Judenhofer M. *et al.*, *Nat. Med.*, **14** (2008) 439.

[52] Berneking A. *et al.*, *IEEE Trans. Nucl. Sci.*, **64** (2017) 1118.

[53] Costa D. N. *et al.*, *Urol. Oncol.: Sem. Orig. Inv.*, **34** (2016) 255.e7.

[54] Gawlitza J. *et al.*, *Sci. Rep.*, **7** (2017) 40640.

[55] Sosna J. *et al.*, *Acad. Radiol.*, **11** (2004) 857.

[56] Rezaei A. *et al.*, *IEEE Trans. Med. Imaging*, **33** (2014) 1563.

[57] Defrise M. *et al.*, *Phys. Med. Biol.*, **59** (2014) 1073.

[58] Mehranian A. and Zaidi H., *IEEE Trans. Med. Imaging*, **34** (2015) 1808.

[59] Rezaei A. *et al.*, *IEEE Trans. Med. Imaging*, **31** (2012) 2224.

[60] Rezaei A. *et al.*, *IEEE Trans. Med. Imaging*, **39** (2020) 952.

[61] Rezaei A. *et al.*, *Maximum Likelihood Estimation of the Geometric Sensitivities*, in *PET
    2019 IEEE Nuclear Science Symposium and Medical Imaging Conference (NSS/MIC)*
    (IEEE) 2019.